Theoretical Raman intensity of the radial breathing mode of single-walled carbon nanotubes

ARTICLE *in* PHYSICA STATUS SOLIDI (B) · NOVEMBER 2007

Impact Factor: 1.49 · DOI: 10.1002/pssb.200776176

2 AUTHORS:

Valentin N. Popov
Sofia University "St. Kliment Ohridski"
114 PUBLICATIONS **3,844** CITATIONS
SEE PROFILE

Philippe Lambin
University of Namur
295 PUBLICATIONS **7,911** CITATIONS
SEE PROFILE

physica status solidi pss b
www.pss-b.com
basic solid state physics

Theoretical Raman intensity of the radial breathing mode of single-walled carbon nanotubes

V. N. Popov[1] and **P. Lambin**[2]

[1] Faculty of Physics, University of Sofia, Sofia, Bulgaria
[2] Laboratoire de Physique du Solide, Facultés Universitaires Notre-Dame de la Paix, Namur, Belgium

Received 29 March 2007, revised 12 June 2007, accepted 21 September 2007
Published online 8 November 2007

PACS 63.22.+m, 73.22.–f, 78.30.Na

The atomistic calculations of the physical properties of perfect single-walled carbon nanotubes can be performed successfully by use of the helical symmetry of the nanotubes. The efficiency of this approach is illustrated by calculations of the electronic band structure, lattice dynamics, and the resonant Raman intensity of the radial-breathing mode for all nanotubes in the diameter range from 0.6 nm to 2.4 nm within a symmetry-adapted nonorthogonal tight-binding model. It is shown that the derived electron–phonon coupling and the Raman intensity are in fair agreement with recent Raman data on individual nanotubes.

phys. stat. sol. (b) **244**, No. 11, 4269–4274 (2007) / **DOI** 10.1002/pssb.200776176

WILEY-VCH

Original Paper

phys. stat. sol. (b) **244**, No. 11, 4269–4274 (2007) / **DOI** 10.1002/pssb.200776176

Theoretical Raman intensity of the radial breathing mode of single-walled carbon nanotubes

V. N. Popov[*, 1] and **P. Lambin**[2]

[1] Faculty of Physics, University of Sofia, Sofia, Bulgaria
[2] Laboratoire de Physique du Solide, Facultés Universitaires Notre-Dame de la Paix, Namur, Belgium

Received 29 March 2007, revised 12 June 2007, accepted 21 September 2007
Published online 8 November 2007

PACS 63.22.+m, 73.22.–f, 78.30.Na

The atomistic calculations of the physical properties of perfect single-walled carbon nanotubes can be performed successfully by use of the helical symmetry of the nanotubes. The efficiency of this approach is illustrated by calculations of the electronic band structure, lattice dynamics, and the resonant Raman intensity of the radial-breathing mode for all nanotubes in the diameter range from 0.6 nm to 2.4 nm within a symmetry-adapted nonorthogonal tight-binding model. It is shown that the derived electron–phonon coupling and the Raman intensity are in fair agreement with recent Raman data on individual nanotubes.

1 Introduction

The successful debundling of the single-walled carbon nanotubes (or, simply, nanotubes) by dissolving and wrapping with organic molecules opened up new possibilities for the investigation of the nanotubes [1]. In particular, significant progress was achieved in the precise resonant Raman measurements of individual nanotubes. Among the most frequently studied Raman features is the line originating from the so-called radial breathing mode (RBM), in which all carbon atoms have uniform radial displacements. The use of tunable lasers allows for the detailed measurement of the excitation profile of the RBM [2, 3].

The theoretical simulations of the Raman intensity of the RBM using general-purpose computational codes are restricted to small sets of nanotube types because of the normally very large unit cells of the nanotubes. However, the explicit use of the screw symmetry of the nanotubes allows for large-scale calculations of the electronic band structure, the phonon dispersion, and the resonant Raman intensity. The verification of the predictions for the Raman intensity can be done by comparing the calculated electron–phonon coupling to the measured one and by comparing the theoretical Raman intensity to the observed one. In the case of agreement with experiment, the predicted Raman intensity can be used for determination of the nanotube distribution in the sample.

Here, we present symmetry-adapted models of the electronic band structure and the phonon dispersion of nanotubes. Based on these models, we derive the optical transition energies, the RBM frequency, and the resonant Raman intensity of the RBM for practically all observable nanotubes. The obtained results are compared to available experimental Raman data. The paper ends with conclusions.

2 Theoretical aspects

The calculations of the electronic band structure and phonon dispersion of systems with translational periodicity use the Bloch theorem to reduce the infinite number of atoms in the system to the unit-cell

[*] Corresponding author: e-mail: vpopov@phys.uni-sofia.bg, Phone: +00 359-2-8161-833, Fax: +00 359-2-9625-276

atoms only. In the matrix formulation of these problems, one has to diagonalize matrices linear in the number of atoms in the unit cell. In the case of the presently synthesized nanotubes, this number can vary from a few up to a few thousand, which makes it practically impossible to solve the electronic and vibrational problems for the majority of the observed nanotubes. This problem can be overcome by considering the screw symmetry of the nanotubes [4–6]. The screw operation consists of a rotation around the nanotube axis and a translation along this axis. For each nanotube, there are two primitive screw operations. By use of linear combinations of these two screw operations, a two-atom unit cell can be mapped onto the entire nanotube. Correspondingly, a generalized Bloch theorem can be proven and the electronic and vibrational problems can be formulated for a two-atom unit cell. Thus, the computational time for solving these problems within such symmetry-adapted approach is drastically reduced, which makes it possible to encompass all nanotubes of practical interest.

The explicit use of the screw symmetry in band-structure calculations will be illustrated in the case of a nonorthogonal tight-binding (NTB) model [7, 8]. One starts with the one-electron Schrödinger equation and expands the one-electron wavefunctions as linear combinations of basis functions, where the basis functions are Bloch sums of atomic orbitals. In the NTB model, we consider all four valence-electron orbitals of the carbon atom. The rotational boundary condition and the translational periodicity condition impose restrictions on the basis wavefunctions, leading to reduction of the graphene two-dimensional wavevector to a one-dimensional wavevector k ($-\pi \le k < \pi$; k is in units of the inverse nanotube primitive translation) and an azimuthal quantum number l ($l = 0, 1, \ldots, N-1$; N is the number of carbon pairs in the unit cell). The substitution of the one-electron wavefunction in the Schrödinger equation yields the generalized matrix eigenvalue problem

$$\sum_{r'} H_{klrr'} c_{klr'} = E_{kl} \sum_{r'} S_{klrr'} c_{klr'} \ . \tag{1}$$

Here, the quantities $H_{klrr'}$ and $S_{klrr'}$ are expressed through the matrix elements of the one-electron Hamiltonian and the overlap integrals, respectively. The index r runs over the atomic orbitals of the two-atom unit cell ($r = 1, 2, \ldots, 8$). The solutions of Eq. (1) are the electron eigenenergies E_{klm} and the expansion coefficients c_{klmr} ($m = 1, 2, \ldots, 8$). For each k, there are $8N$ electronic states but the number of different eigenenergies is smaller because of degeneracy.

A symmetry-adapted dynamical model can be constructed in a similar way as above [9–11]. First, we consider a force-constant model of the lattice dynamics of nanotubes. For small displacements of the atoms from their equilibrium positions, the potential energy of the distorted nanotube is expanded in series of the displacements up to second degree. The atomic displacements are written as Bloch sums with a two-dimensional wavevector. The rotational boundary condition and the translational periodicity condition impose restrictions on the atomic displacements and lead to the replacement of the two-dimensional wavevector with a one-dimensional wavevector q ($-\pi \le q < \pi$) and an azimuthal quantum number l ($l = 0, 1, 2, \ldots, N-1$). The substitution of the atomic displacements in the equations of motion gives the following system of six linear equations

$$\omega^2 e_\alpha(\kappa) = \sum_{\kappa'\beta} D_{\alpha\beta}(\kappa\kappa' \mid ql)\, e_\beta(\kappa') \ . \tag{2}$$

Here, the index κ runs over the atoms of the two-atom unit cell ($\kappa = 1, 2$); α and β are Cartesian coordinate indices. The dynamical matrix $D_{\alpha\beta}$ can be constructed from force constants [9, 10] or derived within the NTB model in the linear-response approximation [11]. The equations of motion, Eq. (2), give the phonon eigenfrequencies ω_{qlj} and eigenvectors $e_{\beta,qlj}(\kappa)$, ($j = 1, 2, \ldots, 6$). For each q, there are $6N$ phonons but the number of different frequencies is smaller because of degeneracy.

Among the various phonons of a nanotube, of major interest is the RBM, which dominates the low-frequency Raman spectra and can be used for characterization of the nanotube samples because of the well-studied $1/R$ dependence of its frequency ω_{RBM} (R is the nanotube radius). The Raman scattering of light from nanotubes is observed exclusively under resonant conditions, i.e. when the laser excitation line

is close to an optical transition energy of a nanotube. This requires a combined consideration of the electronic and phonon subsystems and their interaction. A consistent derivation of the Raman scattering intensity can be done within third-order time-dependent quantum-mechanical perturbation theory [12–14]. The most resonant Stokes process includes an absorption of a photon (energy E_L and polarization $\boldsymbol{\varepsilon}_L$) with creation of an electron–hole pair, scattering of the electron (hole) by the RBM (energy $E_o = \hbar\omega_o$ and eigenvector $\boldsymbol{e}_o$), and annihilation of the electron–hole pair by emission of a photon (energy $E_S = E_L - E_o$ and polarization $\boldsymbol{\varepsilon}_S$). The intensity for this process is given by

$$I(E_L, E_o) = A\left|\frac{1}{L}\sum_{cv}\frac{p_{cv}^{S} M_{cv} p_{cv}^{L*}}{(E_L - E_{cv} - i\gamma_e)(E_S - E_{cv} - i\gamma_e)}\right|^2 . \tag{3}$$

Here, $A = C\,(E_S/E_L)^2\,(n+1)$ with C being a constant, n is the phonon Bose–Einstein factor, L is the tube length, and γ_e is the excited state width. E_{cv} is the energy difference for a given pair of valence (v) and conduction (c) bands and the summation is over all k-vectors and all pairs of cv bands. p_{cv} is the component of the matrix element of the electron momentum in the direction of the incident or scattered photon polarization, calculated between the wavefunctions of a pair of valence and conduction bands. M_{cv} is the electron–phonon matrix element [15]. Later, we shall consider only light polarization along the tube axis, when the momentum matrix elements are nonzero only for pairs of bands with $l = l'$. Obviously, the intensity is resonantly enhanced for E_L or E_S close to a minimum of E_{cv}. Such minima correspond to the optical transition energies and will be denoted by E_{ii} (ii = 11, 22 …).

The expression for the intensity can be simplified by noticing that the dominant contribution to the sum in Eq. (3) comes from k-points around a minimum of E_{cv}. We can pull the numerator out of the summation at the point of the minimum E_{ii} and carry out the remaining summation as integration. The obtained intensity is

$$I(E_L, E_o) = A'\left|\sum_{ii} J_{ii} F_{ii}(E_L, E_o)\right|^2 , \tag{4}$$

where

$$J_{ii} = |p_{ii}|^2\, M_{ii}\sqrt{m_{ii}^*} , \tag{5}$$

$$F_{ii}(E_L, E_o) = \frac{2}{\hbar\omega_o}\left(\frac{1}{\sqrt{E_L - E_{ii} - i\gamma_e}} - \frac{1}{\sqrt{E_S - E_{ii} - i\gamma_e}}\right), \tag{6}$$

$A' = C'\,(E_S/E_L)^2\,(n+1)$ with C' being a constant, m_{ii}^* is the reduced effective mass, and p_{ii} and M_{ii} are the matrix elements at E_{ii}. It is clear that F_{ii} determines the resonance window, i.e. the range of laser energies, for which the intensity is noticeably different from zero, and J_{ii} determines the contribution of a given tube to the Raman intensity. Once J_{ii} are known for all nanotubes in a given range of diameters, one can easily calculate the Raman spectrum of a nanotube sample by summing up the intensity, Eq. (4), over all nanotube types with a weight factor proportional to the nanotube population in the sample.

3 Results and discussion

We used the parameters for the NTB model derived from a density-functional theory study on carbon clusters [16]. This parametrization also includes pairwise interatomic interactions that allows one to calculate the total energy of the system and perform structural relaxation. This is mandatory for phonon calculations, where one should know the equilibrium state of the system.

We calculated the electronic band structure and optical transitions for all nanotubes in the radius range from 2 Å up to 12 Å [7, 8]. The obtained optical transitions compare well to partial density-functional results available on a limited sets of nanotubes (e.g., [17]). The NTB optical transitions correspond well

to the observed ones but require roughly a rigid upshift correction of about 0.3 eV [13] to account for the self-energy and excitonic effects [18]. Recent experimental Raman data has suggested a rigid upshift correction of about 0.43 eV for optical transitions with $ii > 22$, which questions the exciton binding for such optical transitions [19–22]. Detailed analysis of the upshift correction has been performed in Ref. [23]. The corrected NTB E_{ii}'s can be used for characterization of nanotube samples by means of Raman spectroscopy. Later, similar symmetry-adapted NTB models were reported independently [24] or using the approach presented here [25]. Symmetry-based density-functional calculations were accomplished for a few tens of nanotubes [26, 27]. We note that the single-electron approximation may not be adequate for some phenomena and then one should use a more complicated description of the optical transitions in terms of excitons [28].

We performed large-scale calculations of the zone-center phonons and the phonon dispersion of all nanotube types in the radius range as above. The dynamical matrix was calculated within a valence-force-field model [9], force-constant model [10], and NTB model in the linear-response approximation [11]. As is typical for the tight-binding models, the predicted RBM frequency overestimates the experimental values and has to be downscaled by a factor of 0.9 [11]. Other symmetry-based dynamical models have been reported as well [29, 30].

We carried out large-scale NTB calculations of the Raman intensity of the RBM for all nanotube types as above [12–14]. Later, similar results were reported for a one-orbital tight-binding model [31] or for the same NTB model but with electron-phonon coupling estimated with one orbital per carbon atom [32]. All these calculations of the Raman intensity are based on the single-particle approximation, while experiment suggests an excitonic nature of the lower-energy optical transitions. We do not consider here partial predictions of the intensity within the exciton picture because for the moment they are insufficient for comparison with experimental data (see below) and for verification of their validity.

The electron–phonon coupling (squared) has been obtained from the ratio of the intensity of the one- and two-phonon Raman lines of individual nanotubes for the second semiconducting transition E_{22} [33–35]. In the first two cited papers, a very good agreement was found between the experimental ratios and the estimated couplings [13, 39], while in the third paper disagreement of up to a factor of three can be observed irrespective of the model used (NTB or quantum-chemical excitonic calculations) (see Fig. 1).

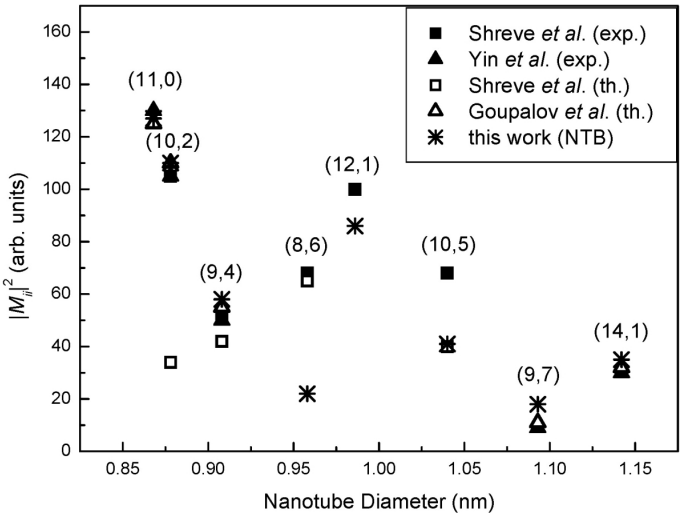

Fig. 1 Experimental squared electron–phonon coupling for several nanotubes in comparison with theoretical estimations. The experimental data [35, 34] (solid symbols) was upshifted for coincidence of the points for nanotube (10,2). The theoretical data [39] (empty symbols) and [13] (stars) were scaled for best fit to the experimental ones.

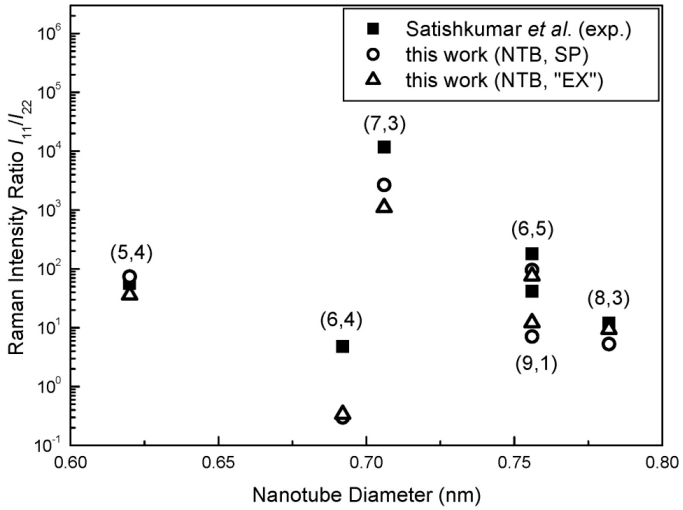

Fig. 2 Experimental ratio of the Raman intensities for the first and second optical transitions [38] (solid symbols) in comparison with theoretical results [13] (empty symbols). The notation "SP" stands for single particle results and "EX" stands for "excitonic" calculations, which use excitonic Raman line shape and single-particle matrix elements. The latter calculations do not improve the agreement with experiment.

The predicted Raman intensities can be used for simulation of Raman spectra of samples with known nanotube distribution. In the case of an assumed Gaussian diameter distribution [36], the predicted Raman spectra for three laser lines showed fair agreement with the experimental ones [12]. More accurate conclusions can be drawn on data for individual nanotubes by comparing the ratios of the intensities for two optical transitions. The experimental ratio of the intensities I_{11} and I_{22} for the metallic nanotube (10,4) was found to be around 6 [37], while the NTB model gives 7.26 [32] and about 320 [13]. In another Raman measurement of the excitation profile for the first and second optical transitions of the semiconducting nanotubes (5,4), (6,4), (7,3), (6,5), (9,1), and (8,3) [38], the predicted ratio of the intensities I_{11}/I_{22} [13, 39] corresponds fairly well to the experimental ones within up to one order of magnitude (Fig. 2). Noticing that the order of magnitude of this ratio varies from one to four, we accept such discrepancy as quite acceptable for a semiquantitative model as the used NTB model.

4 Conclusions

We showed that the symmetry-adapted approach allows for the calculation of the electronic band structure, the phonon dispersion, and the Raman intensity of any carbon nanotube of practical interest. The results for the electron–phonon coupling and the intensity are in fair agreement with available experimental data. We believe that a better description of the Raman intensity is possible within the excitonic picture.

Acknowledgements V.N.P. was partly supported by a Marie-Curie Intra-European Fellowship MEIF-CT-2003-501080.

References

[1] S. M. Bachilo, M. S. Strano, C. Kittrell, R. H. Hauge, R. E. Smalley, and R. B. Weisman, Science **298**, 2361 (2002).
[2] C. Fantini, A. Jorio, M. Souza, M. S. Strano, M. S. Dresselhaus, and M. A. Pimenta, Phys. Rev. Lett. **93**, 147406 (2004).
[3] H. Telg, J. Maultzsch, S. Reich, F. Hennrich, and C. Thomsen, Phys. Rev. Lett. **93**, 177401 (2004).

[4] C. T. White, D. H. Robertson, and J. W. Mintmire, Phys. Rev. B **47**, 5485 (1993).
[5] J. W. Mintmire and C. T. White, Carbon **33**, 893 (1995).
[6] M. Damnjanovic, I. Milosevic, T. Vukovic, and R. Sredanovic, Phys. Rev. B **60**, 2728 (1999).
[7] V. N. Popov, New J. Phys. **6**, 17 (2004).
[8] V. N. Popov and L. Henrard, Phys. Rev. B **70**, 115407 (2004).
[9] V. N. Popov, V. E. Van Doren, and M. Balkanski, Phys. Rev. B **61**, 3078–3084 (2000).
[10] Z. M. Li, V. N. Popov, and Z. K. Tang, Solid State Commun. **130**, 657–661 (2004).
[11] V. N. Popov and Ph. Lambin, Phys. Rev. B **73**, 085407 (2006).
[12] V. N. Popov, L. Henrard, and Ph. Lambin, Nano Lett. **4**, 1795 (2004).
[13] V. N. Popov, L. Henrard, and Ph. Lambin, Phys. Rev. B **72**, 035436 (2005).
[14] V. N. Popov and Ph. Lambin, Phys. Rev. B **73**, 165425 (2006).
[15] V. N. Popov and Ph. Lambin, Phys. Rev. B **74**, 075415 (2006).
[16] D. Porezag, Th. Frauenheim, and Th. Köhler, Phys. Rev. B **51**, 12947 (1995).
[17] M. Machón, S. Reich, C. Thomsen, D. Sánchez-Portal, and P. Ordejón, Phys. Rev. B **66**, 155410 (2002).
[18] C. L. Kane and E. J. Mele, Phys. Rev. Lett. **93**, 197402 (2004).
[19] G. Dukovic, F. Wang, D. Song, M. Y. Sfeir, T. F. Heinz, and L. E. Brus, Nano Lett. **5**, 2314 (2005).
[20] M. Paillet, T. Michel, J. C. Meyer, V. N. Popov, L. Henrard, S. Roth, and J.-L. Sauvajol, Phys. Rev. Lett. **96**, 257401 (2006).
[21] A. Jungen, V. N. Popov, C. Stampfer, L. Durrer, S. Stoll, and C. Hierold, Phys. Rev. B **75**, 041405(R) (2007).
[22] T. Michel, M. Paillet, J. C. Meyer, V. N. Popov, L. Henrard, and J.-L. Sauvajol, Phys. Rev. B **75**, 155432 (2007).
[23] P. T. Araujo, S. K. Doorn, S. Kilina, S. Tretiak, E. Einarsson, S. Maruyama, H. Chacham, M. A. Pimenta, and A. Jorio, Phys. Rev. Lett. **98**, 067401 (2007).
[24] I. Milošević, B. Nikolić, and M. Damnjanović, Phys. Rev. B **69**, 113408 (2004).
[25] Ge. G. Samsonidze, R. Saito, N. Kobayashi, A. Grüneis, J. Jiang, A. Jorio, S. G. Chou, G. Dresselhaus, and M. S. Dresselhaus, Appl. Phys. Lett. **85**, 5703 (2004).
[26] I. Cabria, J. W. Mintmire, and C. T. White Phys. Rev. B **67**, 121406 (2003).
[27] F. Bogár, J. W. Mintmire, F. Bartha, T. Mező, and C. V. Alsenoy, Phys. Rev. B **72**, 085452 (2005).
[28] E. Chang, G. Bussi, A. Ruini, and E. Molinari, Phys. Rev. Lett. **92**, 196401 (2004).
E. Chang, G. Bussi, A. Ruini, and E. Molinari, Phys. Rev. B **72**, 195423 (2005).
[29] E. Dobardžić, I. Milošević, B. Nikolić, T. Vuković, and M. Damnjanović, Phys. Rev. B **68**, 045408 (2003).
[30] G. D. Mahan and G. S. Jeon, Phys. Rev. B **70**, 075405 (2004).
[31] S. V. Goupalov, Phys. Rev. B **71**, 153404 (2005).
[32] J. Jiang, R. Saito, Ge. G. Samsonidze, S. G. Chou, A. Jorio, G. Dresselhaus, and M. S. Dresselhaus, Phys. Rev. B **72**, 235408 (2005).
[33] Z. Luo, F. Papadimitrakopoulos, and S. K. Doorn, Appl. Phys. Lett. **88**, 073110 (2006).
[34] Y. Yin, A. N. Vamivakas, A. G. Walsh, S. B. Cronin, M. S. Ünlü, B. B. Goldberg, and A. K. Swan, Phys. Rev. Lett. **98**, 037404 (2007).
[35] A. P. Shreve, E. H. Haroz, S. M. Bachilo, R. B. Weisman, S. Tretiak, S. Kilina, and S. K. Doorn, Phys. Rev. Lett. **98**, 037405 (2007).
[36] S. K. Doorn, D. A. Heller, P. W. Barone, M. L. Usrey, and M. S. Strano, Appl. Phys. A **78**, 1147 (2004).
[37] H. Son, A. Reina, Ge. G. Samsonidze, R. Saito, A. Jorio, M. S. Dresselhaus, and J. Kong, Phys. Rev. B **74**, 073406 (2006).
[38] B. C. Satishkumar, S. V. Goupalov, E. H. Haroz, and S. K. Doorn, Phys. Rev. B **74**, 155409 (2006).
[39] S. V. Goupalov, B. C. Satishkumar, and S. K. Doorn, Phys. Rev. B **73**, 115401 (2006).

